

CEPAS 2017

7th Conference on Elementary Processes in Atomic Systems



3rd – 6th September 2017

Průhonice, Czech Republic



Table of Contents

Programme	3
List of Posters	5
Abstracts of Oral Contributions	7
Abstracts of Posters	29
List of Participants	59

Local organizing comitee:

Václav Alt
Martin Čížek
Roman Čurík
Karel Houfek
Dávid Hvizdoš
Michal Tarana
Petra Votavová



International scientific committee:

Friedrich Aumayr, Austria
Joachim Burgdorfer, Austria
Robert DuBois, United States
Gustavo Garcia Gomez-Tejedor, Spain
Jiří Horáček, Czech Republic
Bratislav P. Marinkoviá, Serbia
Nigel J. Mason, United Kingdom
Ladislau Nagy, Romania
Zoran Lj. Petrović, Serbia
Otto B. Shpenik, Ukraine
Andrey Solovyov, Germany
Viorica Stancalie, Romania
John A. Tanis, United States
Károly Tókesi, Hungary
Mariusz Zubek, Poland

Editors: Michal Tarana, Roman Čurík

First published: September 2017

Published by:

J. Heyrovský Institute of Physical Chemistry, v.v.i.
Academy of Sciences of the Czech Republic
Dolejškova 3, 18223 Prague 8
Czech Republic



ISBN 978-80-87351-46-8

Programme

Sunday, September 3

15:00 Registration

19:00 Opening and welcome reception

Monday, September 4

Photoionization and photoemission - *Chairman: Bratislav Marinković*

9:00 Fernando Martín Attochemistry: Imaging and controlling electron dynamics in molecules (*Page 9*)

9:45 Ticia Buhr Azimuth angle dependence of the He 1s and Ne 2s photoelectron angular distributions (*Page 10*)

10:10 Coffee break

10:40 Paola Bolognesi Radiation damage in systems of biological interest: the case of radiosensitisers (*Page 11*)

11:25 Alexei Grum-Grzhimailo Coherent control of electron emission in short-pulse XUV atomic ionization (*Page 12*)

11:50 Andrej Bunjac Calculation of the dynamic Stark shift for sodium and the application to resonantly enhanced multiphoton ionization (*Page 13*)

12:15 Lunch

Electron and photon interactions - *Chairman: Martin Čížek*

14:00 Petr Dohnal Laboratory study of electron-ion recombination and of associative detachment at low temperatures (*Page 14*)

14:25 Roman Čurík Inelastic low-energy collisions of electrons with small cations (*Page 15*)

14:50 Petra Votavová Superexchange Interatomic Coulombic decay by Fano-ADC-Stieltjes method (*Page 16*)

15:15 Viorica Stancalie Studies of the electron-correlation and relativistic effects in target representation and low-energy collision calculations (*Page 17*)

15:40 Coffee break

16:15 Poster Session, International Scientific Committee meeting

19:00 Individual dinner

Tuesday, September 5Ion interactions - *Chairman: Robert DuBois*

- 9:00 Alicja Domaracka Ion collisions with complex molecular systems: isolated molecules, clusters and astrophysical ices (*Page 18*)
- 9:45 Sándor Kovács Dissociative ionization of H₂O molecule bombarded by single charged projectiles (*Page 19*)
- 10:10 Coffee break
- 10:40 Jeff Shinpaugh Experimental and computational study of gold nanoparticles as a radiosensitizer for proton radiation (*Page 20*)
- 11:25 François Frémont Classical treatment of autoionization in slow ion-atom collisions (*Page 21*)
- 11:50 Nikolaus Stolterfoht Milestones of highly charged ion guiding through insulating capillaries: applications to a conical shape (*Page 22*)
- 12:15 Lunch
- 14:20 Departure to Prague, Excursion
- 19:00 Conference Dinner in the Strahov Monastery Brewery

Wednesday, September 6Electron-impact experiments - *Chairman: Gustavo García*

- 9:00 Janina Kopyra Low energy electron driven decomposition of biologically relevant molecules (*Page 23*)
- 9:45 Marián Danko Dissociative ionization of cyclopropylamine (*Page 24*)
- 10:10 Coffee break
- 10:40 Paulo Limão-Vieira Decomposition of nitroimidazoles by electron impact (*Page 25*)
- 11:25 Jaroslav Kočíšek Does pinene stabilize water aerosols? (*Page 26*)
- 11:50 Nigel Mason Electron driven chemistry on comet 67P observed by Rosetta space craft and its implications (*Page 27*)
- 12:15 Lunch
- 14:00 Departures or individual afternoon in Prague

List of Posters

P-1	<i>Václav Alt</i>	Low-energy resonant electron collisions with O ₂	31
P-2	<i>Ticía Buhr</i>	Absolute cross sections for photoionization of Ne ⁺ ions and Ne atoms in the vicinity of the K-shell ionization threshold	32
P-3	<i>Martin Čížek</i>	Isotope effect in water formation by associative detachment	33
P-4	<i>Sándor Demes</i>	Elastic electron scattering by the CF ₃ radical and by the CF ₃ Cl, CF ₄ molecules in the IAM approach	34
P-5	<i>Sándor Demes</i>	IAM approach study of elastic electron scattering by the CF ₂ , CF ₂ Cl and CF ₃ molecular systems	35
P-6	<i>Sándor Demes</i>	Double electron capture by the O ₂ ⁺ projectile in collisions with the H ₂ molecule	36
P-7	<i>Sándor Demes</i>	Dissociative electron attachment (0-9 eV) to D-ribose molecule	37
P-8	<i>Sándor Demes</i>	Electron impact excitation of the gas-phase ribose molecule	38
P-9	<i>Robert DuBois</i>	Ion guiding through a macroscopic capillary: A quantitative study	39
P-10	<i>Gustavo García</i>	Electron scattering cross section data for tungsten and beryllium atoms from 0.1 to 5000 eV	40
P-11	<i>Dávid Hvizdoš</i>	Analysis of two theoretical methods for dissociative recombination of small cations	41
P-12	<i>Zoltán Juhász</i>	Thermodynamic model of molecular collisions	42
P-13	<i>Jaroslav Kočíšek</i>	DNA binding radiosensitizers and low energy electrons	43
P-14	<i>Sándor Kovács</i>	Electron emission mechanisms in ion-induced ionization of small molecules	44
P-15	<i>Bratislav Marinković</i>	Nd:YAG laser ablation of materials of biological interest	45
P-16	<i>Bratislav Marinković</i>	Ejected electron spectra from Coster-Kronig transitions in argon	46
P-17	<i>Bratislav Marinković</i>	Electron transmission through steel capillary	47
P-18	<i>Dušan Mészáros</i>	Low energy electron attachment to C ₃ F ₈ , C ₄ F ₈ molecules and clusters	48
P-19	<i>Marek Moneta</i>	PIXE induced by medium energy heavy ions in application to analysis of thin films and subsurface regions	49
P-20	<i>Marek Moneta</i>	Photophysical and structural properties of quinoxalinophenanthrophenazines thin films	50
P-21	<i>Béla Paripás</i>	High resolution study of the autoionizing states of He in the vicinity of the equal velocity region	53
P-22	<i>Béla Paripás</i>	Classical Trajectory Monte Carlo simulation of coincidence experiments in electron impact ionization of helium	54
P-23	<i>Miloš Ranković</i>	VUV action spectroscopy of protonated Tri-Alanine peptide	55
P-24	<i>John Tanis</i>	Radiative double electron capture in F ₉ ⁺ +N ₂ and Ne collisions	56
P-25	<i>Sanja Tosić</i>	The photofragmentation of the core excited halothane molecule	57

Nd:YAG laser ablation of materials of biological interest

M.S. Rabasović¹, D. Sević¹, B.P. Marinković¹

¹*Institute of Physics Belgrade, University of Belgrade, Serbia*

The aim of this study is to analyze the possibilities of using of the Laser Induced Breakdown Spectroscopy (LIBS) for discerning the materials ablated by laser. Lasers are widely used for ablation of biological materials. For practical considerations in biomedical applications, it is necessary to have a real-time feedback control system, so that discriminating between the ablated layers is possible. As excitation laser we use Nd:YAG (1064 nm, pulse width 5 ns, energy up to 300 mJ). We used dry pork bone as an experimental sample. The diagnostic part of our experiment is based on streak camera, so we can perform the time resolved analysis of spectral data. Reasoning of our LIBS analysis follows the concept presented in [1], where femtosecond laser was used for tissue ablation. Sodium (Na) line at 589 nm and Calcium (Ca) line at 612 nm could be used for discrimination between the soft tissue and the bone. Nanosecond Nd:Yag lasers are also widely used for biomedical applications [2,3] Our method of time resolved LIBS is presented in [4]. This study was inspired by a similar analysis (not for biological

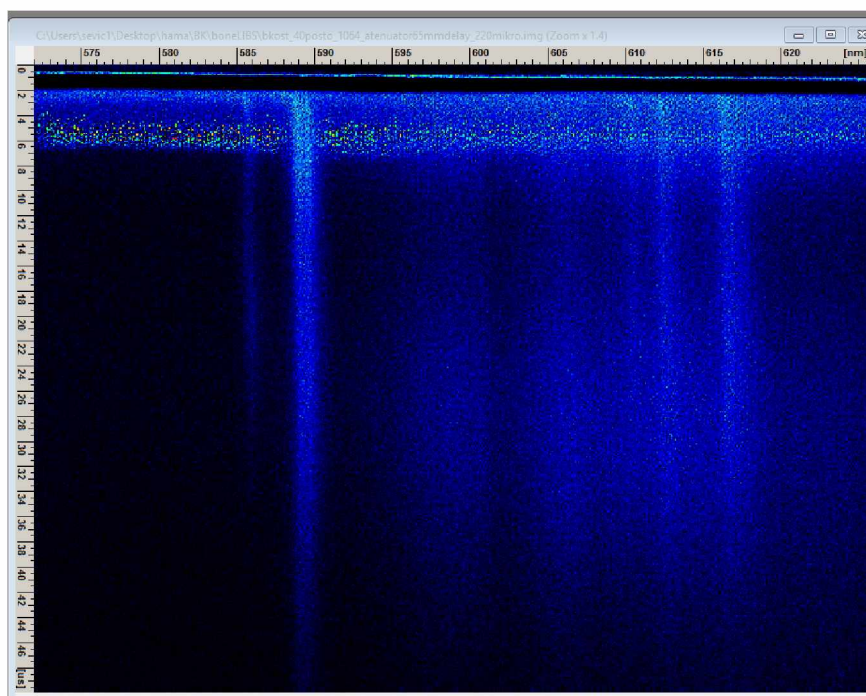


Figure 1: Streak image of LIBS of a dry bone.

materials, but for printed circuit board) presented in [5]. The real application would be based on using the simpler, not time resolved spectrograph with gated acquisition time frame. Our analysis of streak images provides the proof of the concept. Also, the optimal value of gate time is determined by our analysis.

- [1] R.K. Gill *et al.*, *J. J. Biophotonics* **9** (2016) 17.
- [2] B. Cencic *et al.*, *Appl. Phys. A* **112** (2013) 65.
- [3] G. Hawlina *et al.*, *BMC Ophthalmology* **14** (2014) 131.
- [4] M.S. Rabasovic *et al.*, *IEEE Trans. Plasma Sci.* **42** (2014) 2588.
- [5] M.S. Rabasovic *et al.*, *Appl. Phys. A*, **122** (2016) 186.

Ejected electron spectra from Coster-Kronig transitions in argon

B.P. Marinković¹, J.J. Jureta¹, L. Avaldi²

¹Laboratory for Atomic Collision Processes, Institute of Physics Belgrade, University of Belgrade, Pregrevica 118, 11080 Belgrade, Serbia

²CNR-Istituto di Struttura della Materia, Area della Ricerca di Roma 1, CP10, 00015 Monterotondo Scalo, Italy

High resolution ejected electron spectroscopy has been used to investigate ejected electrons in the energy region of the Coster-Kronig (C-K) transitions from 25 to 56 eV in Ar at incident electron energies of 243, 324, 606, 909 and 2018 eV and fixed ejection angle of 90°. The C-K spectrum in Ar includes transitions from the initial state $1s^2 2s 2p^6 3s^2 3p^6$ to the final states $1s^2 2s^2 2p^5 3s(^1P, ^3P) 3p^6$, and $1s^2 2s^2 2p^5 3s^2 3p^5(^3D, ^1D, ^3S, ^1S)$ [1]. In the C-K process the vacancy in the 2s shell (L_1) made by the impact of electrons with energies larger than 327 eV is filled by an electron from the 2p subshells ($L_{2,3}$), while the second electron from either 3s or 3p subshells ($M_1, M_{2,3}$) is promoted to the continuum. The final result is formation of two separate groups of peaks around 30 and 50 eV i.e. ($L_1-L_{2,3}M_1$) and ($L_1-L_{2,3}M_{2,3}$) respectively.

The intensity evolution of all states in the C-K energy region was studied at several incident electron energies from 243 to 2018 eV. The calibration of ejected energy scale was made with respect to the energy position of the Ar $3d(^1D)$ state at 11.72 eV measured under the same experimental conditions.

The measurements have been carried out using a crossed electron-atom beam apparatus OHRHA [2] equipped with an electron gun that can be rotated around the axis of the electrostatic lenses of the analyzer, and the hemispherical analyzer with 7 channeltrons as detectors. The energy resolution of the ejected electron spectra measured as full width at half maximum (FWHM) of the narrowest feature in the spectrum, was typically between 60 and 80 meV.

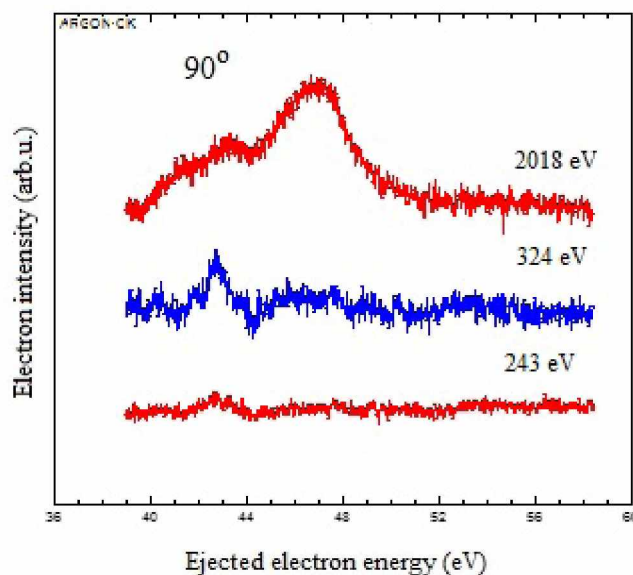


Figure 1: Coster – Kronig transition lines in Ar obtained at 243, 327 and 2018 eV incident electron energies and ejection angle of 90°.

[1] T. Kylli *et al.*, Phys. Rev. A **59** (1999) 4071.

[2] J.J.Jureta *et al.*, Int.J.Mass Spectrom. **114** (2014) 365.

Electron transmission through steel capillary

B.P. Marinković¹, M.Lj. Ranković¹, J.B. Maljković¹, A.R. Milosavljević², D. Borka³, C. Lemell⁴, K. Tökesi⁵

¹*Institute of Physics Belgrade, University of Belgrade, Pregrevica 118, 11080 Belgrade, Serbia*

²*PLÉIADES beamline, Synchrotron SOLEIL, L'orme des Merisiers, Saint-Aubin - BP48, 91192 GIF-sur-YVETTE CEDEX, France*

³*Atomic Physics Laboratory, Vinča Institute of Nuclear Sciences, University of Belgrade, Belgrade, Serbia*

⁴*Institute for Theoretical Physics, Vienna University of Technology, Vienna, Austria*

⁵*Institute for Nuclear Research, Hungarian Academy of Sciences (ATOMKI), Debrecen, Hungary and ELI-ALPS, ELI-HU Non-profit Kft., Szeged, Hungary*

The transmission of low-energy electrons through platinum [1, 2] and steel capillaries have been investigated both experimentally and theoretically. The length of the present steel capillary was $L = 19.50$ mm while the inner diameter was $d = 0.90$ mm. Kinetic energy distribution of electrons transmitted through steel capillary was recorded at two tilt angles (the angle between the incident electron beam and the capillary axis) of 2.64° and 4.0° , respectively. The experimental results were obtained by an electron spectrometer which consists of an electron gun, a double cylindrical mirror energy analyzer (DCMA) and a channeltron detector.

Electron transmission is modelled by a classical trajectory Monte Carlo simulation taking both elastic and inelastic scattering events of primary electrons colliding with the inner wall of the capillary and transport of secondary electrons into account.

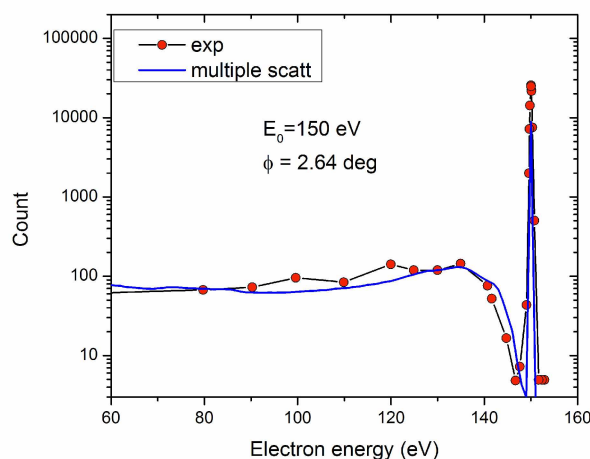


Figure 1: Energy spectra of electrons transmitted through a steel capillary.

Figure 1 shows energy spectra of 150 eV electrons passing through the steel capillary at 2.64° tilt angle. We found excellent agreement between our simulated electron-energy spectra with experimental data.

[1] A.R. Milosavljević *et al.*, Nucl. Instr. Meth. Phys. Res. B **354** (2015) 86.

[2] D. Borka *et al.*, Nucl. Instr. Meth. Phys. Res. B, in press (2017), <http://dx.doi.org/10.1016/j.nimb.2017.02.024>

High resolution study of the autoionizing states of He in the vicinity of the equal velocity region

B. Paripás¹, J.J. Jureta², B. Palásthy¹, B.P. Marinković², G. Pszota¹

¹*Institute of Physics, University of Miskolc, 3515 Miskolc-Egyetemváros, Hungary*

²*Laboratory for Atomic Collision Processes, Institute of Physics Belgrade, University of Belgrade, Pregrevica 118, 11080 Belgrade, Serbia*

By “equal velocity region” we mean the primary electron energy range in which the energies of the autoionizing electrons approximately match that of the scattered electrons. This range is around 90-95 eV for the four most important autoionizing states of helium. Then such interesting phenomena can occur as the post-collision interaction and certain types of the state-to-state interference. We have been studying this range for a long time [1], concentrating the interference of the $2s^2(^1S)$ and $2p^2(^1D)$ resonances. It takes place at 93.15 eV critical primary energy, where the energy of the scattered electron from one reaction path equals the energy of the ejected (autoionizing) electron released along the other path and vice versa: here the scattered-ejected electron pairs are indistinguishable. The observation of this exchange interference is disturbed by the Fano interference (the interference between the direct and indirect ionization), too, which occurs at all primary energies. We intend to study it separately in the neighbourhood of the critical energy, and then to estimate its measure for the critical energy.

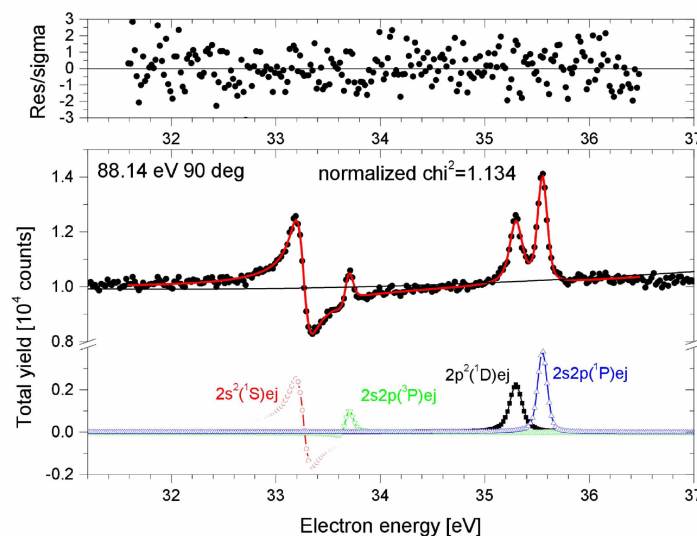


Figure 1: The electron spectrum measured at 90° ejection angle at 88.14 eV primary energy with the best computer fit (solid line). At the bottom the spectrum components, at the top the residuals (in sigma units) are shown.

The present measurements were made by an Omicron High Resolution Hemi-spherical Analyzer (OHRHA) [2] at 88 eV and 97 eV primary energies (where the groups of the ejected and the scattered electron peaks are well separated), at 130° , 90° and 50° ejection angles. The measured spectra were evaluated by a computer code, using the Shore parametrization.

[1] B. Paripás *et al.*, Eur. Phys. J. D **69** (2015) 34.

[2] J.J. Jureta *et al.*, Int. J. Mass Spectr. **114** (2014) 365.

The photofragmentation of the core excited halothane molecule

S.D. Tošić¹, M. Radibratović², M. Milčić³, P. Bolognesi⁴, L. Avaldi⁴, R. Richter⁵, M. Coreno^{4,5}, B.P. Marinković¹

¹*Institute of Physics Belgrade, University of Belgrade, Pregrevica 118, 11080 Belgrade, Serbia*

²*Institute of Chemistry, Technology and Metallurgy – Center for Chemistry, University of Belgrade, Njegoševa 12, 11000 Belgrade, Serbia*

³*University of Belgrade, Faculty of Chemistry, Studentski trg 16, Belgrade, Serbia*

⁴*Istituto di Struttura della Materia-CNR (ISM-CNR), Area della Ricerca di Roma 1, Monterotondo Scalo, Italy*

⁵*Elettra-Sincrotrone Trieste, Area Science Park, I-34012 Basovizza, Trieste, Italy*

In recent years, great attention has been paid to halogenated anesthetics and their role in the destruction of the earth's ozone layer [1]. One of the most commonly used is halothane (C₂HBrClF₃). Compared to the other volatile anesthetics from the same group (halogenated chlorofluorocarbons) this bromide-containing agent is the most destructive against ozone.

We present both experimental and theoretical results related to the photofragmentation of the core-excited halothane molecule. The experiments have been performed at the Gas Phase photoemission beamline of the Elettra synchrotron radiation source (Trieste, Italy) using photons near the C 1s ionization edge (~ 300 eV). The mass spectrum [as shown in Fig.1] is dominated by lighter mass fragments.

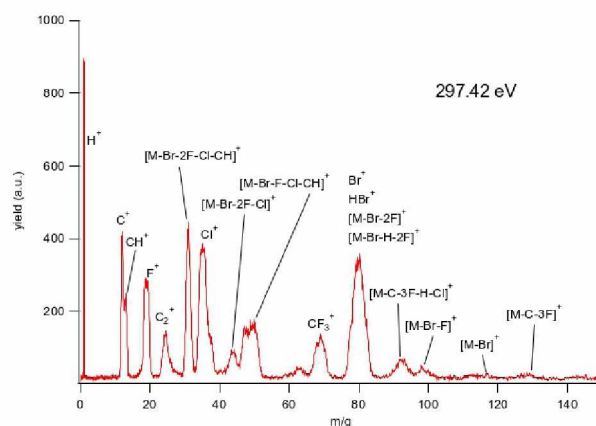


Figure 1: The fragmentation mass spectra of halothane.

To explain the observed large number of lighter mass fragments extensive molecular dynamics (MD) simulations of C₂HBrClF₃²⁺ ion at different temperatures were performed. All MD simulations were carried out in the microcanonical (NVE) ensemble using Verlet algorithm for time integration. At each step of the simulation the potential energy was calculated by minimizing the electronic energy with self-consistent charge-density-functional tight-binding (SCC-DFTB) method as implemented in the DFTB+ code [2]. The results of MD simulations have confirmed the experimental findings: there are fragmentation paths producing almost all fragments found in the mass spectra. For the main fragmentation pathways the minima and the transition states on the potential energy surface were calculated with more accurate quantum chemical methods.

Work partially supported by the MAECI Serbia–Italy Joint Research Project “A nanoview of radiation-biomatter interaction” and the MESTDRS (OI 171020, OI 172065).

[1] A.C. Brown *et al.*, Nature **341** (1989) 635.

[2] B. Aradi *et al.*, J. Phys. Chem. A **111** (2007) 5678.